

# **A Laminated Track for the Inductrack System: Theory and Experiment**

J. F. Hoburg, Carnegie Mellon University, Pittsburgh, PA 15213, USA  
412-268-2473, hoburg@ece.cmu.edu

R. F. Post, Lawrence Livermore National Laboratory, Livermore, CA USA  
925-422-9853, post3@llnl.gov

## **Keywords**

**Halbach arrays**  
**Inductrack**  
**Laminated track**  
**Litz cable track**  
**Urban maglev**

## **Abstract**

This paper describes work on alternative technologies associated with an urban maglev system that employs Halbach arrays of permanent magnets onboard a moving vehicle to induce levitating currents in a stationary “track”. A laminated structure, composed of stacks of thin conducting sheets, has several advantages over a litz-cable ladder as the track. Modeling and experimental results for the laminated track are described and evaluated in this paper.

## **1 Introduction**

As a part of the development of a generic urban maglev system based on the Inductrack approach, studies have been underway at Carnegie-Mellon University and at the Lawrence Livermore National Laboratory on a new kind of maglev track design – the “laminated track”. The laminated track configuration, as its name implies, is composed of a multi-layer laminate made up of thin conducting sheets of copper or aluminum that are slotted transversely, with a slot width that is less than the total width of the sheet. The pattern thus produced can be visualized as a close-packed configuration of shorted electrical circuits within which currents are induced by the passage of the Halbach arrays of the Inductrack maglev configuration. The advantages of the laminated track over the presently employed ladder-like litz-cable design are the higher conductor “packing fraction” that can be achieved, its potentially lower fabrication cost, and the track’s long-time durability (no solder-joints are required in manufacturing the track).

The particular studies reported here are aimed at evaluating the levitation and drag forces of a laminated track. Two approaches to the analysis are discussed: (1) an approach based on 2-D analytic approximations to the 3-D fields of the Halbach arrays, plus a “circuit-based” analysis of the track electromagnetic parameters (R. F. Post), and (2) a “fields-based” approach (J. F. Hoburg) employing Maxwell’s equations, with Fourier analysis of the 3-D field structure and retention of only the first Fourier component. Both approaches were compared to the results of experiments performed on the “Laminated Track Test Rig” constructed at Livermore. Good agreement was found, both between the computed results from the two methods of analysis, and with the results from the test rig.

## 2 Circuit-based analytic description

### 2.1 Calculation of Induced currents, lift and drag

For the purpose of developing a fast-computing Inductrack levitation code, based on a 2-D analytic formulation, we have developed a code, using the Mathematica® platform, that calculates the lift and drag of a laminated track configuration coupling to an Inductrack II double Halbach array levitating system. In writing the code several approximations were made, and it is important to determine the level of error to be expected in the use of these approximations. Our checkpoints include: (1) a “fields-based” description covered in Section 4 of this paper, (2) separate 3-D Halbach array magnetic field calculations based on the Biot-Savart Law and Amperian currents, and (3) experimental results from a “Laminated Track Test Rig” built at the Lawrence Livermore National Laboratory for the express purpose of bench-marking the code. As will be shown, the results from the simple 2-D code track well with results from the Laminated Track Test Rig and with the results of the fields-based treatment in regimes that are of practical interest.

The starting points for the 2-D analysis and code development are the 2-D equations for the vertical (y) and horizontal (x) components of the magnetic field from a single-sided Halbach array, as defined by Halbach in his published work [1]. These are as follows:

$$B_x = B_0 \sin[kx] \exp[-k(y_1 - y)] \quad (1)$$

$$B_y = B_0 \cos[kx] \exp[-k(y_1 - y)] \quad (2)$$

$$B_0 = B_r [1 - \exp(-kd)] \frac{\sin(\pi/M)}{\pi/M} \quad (3)$$

Here, in Equations 1 and 2,  $k = 2\pi/\lambda$ , where  $\lambda$ (m) is the wavelength of the Halbach array,  $y_1$  (m) is the distance between the surface of the Halbach array and the location of a surface current in the track. In Equation 3,  $B_r$  (Tesla) is the remanent field of the magnetic material in the Halbach array,  $d$  (m) is the vertical thickness of the array magnets, and  $M$  is the number of magnet bars per wavelength in the Halbach array.

The magnetic field components (in 2-D approximation) from a dual-Halbach-array (Inductrack II) configuration are simply the superposition of the width-truncated 2-D fields of an upper and lower array, with width and/or thickness dimensions reflecting the particular configuration being considered. In this paper we will be mainly discussing a particular array, the so-called “(5 x 3)” array. That is, a dual array in which the upper array is 5 units wide and the lower array is 3 units wide, with both arrays having the same thickness in the vertical direction. The reason for the unequal widths of the upper and lower arrays is that in this way one achieves a partial nulling of the vertical field component so as to reduce the amount of current induced in the track (relative to the levitating (horizontal) field component when the midplane of the laminated track conductors is located midway between the upper and lower arrays, better to optimize the lift-to-drag ratio at urban speeds. At the same time the magnitude of the horizontal field is increased by the presence of the lower array, thus reducing the amount of current required to levitate a given mass per unit area.

Using Equations (1) and (2) the resultant field components for an Inductrack II magnet configuration with unequal widths of the upper and lower arrays are given by Equations 4, 5, 6, and 7. Here  $w_U$  (m) is the width of the upper array in the  $z$  direction,  $w_L$  (m) is the width of the lower array, and  $v$  (m/sec) is the velocity of the moving Halbach array.

Domain:  $-(w_L/2) < z < (w_L/2)$ :

$$\Sigma B_{y1} = -B_0 \{ \text{Exp}[-k(y_1 - y)] - \text{Exp}[-k(y_1 + y)] \} \text{Cos}[k(x - vt)] \quad (4)$$

$$\Sigma B_{x1} = B_0 \{ \text{Exp}[-k(y_1 - y)] - \text{Exp}[-k(y_1 + y)] \} \text{Sin}[k(x - vt)] \quad (5)$$

Domain:  $-(w_U/2) < -(w_U/2)$  or  $(w_L/2) < (w_U/2)$ :

$$\Sigma B_{y2} = -B_0 \text{Exp}[-k(y_1 - y)] \text{Cos}[k(x - vt)] \quad (6)$$

$$\Sigma B_{x2} = B_0 \text{Exp}[-k(y_1 - y)] \text{Sin}[k(x - vt)] \quad (7)$$

Equations 4 and 5 may now be used to calculate the flux through an area equal to that of an elementary circuit of the laminated track at vertical position  $y_1$ , and from this flux the current induced in that circuit may be determined. The equation for the time-varying flux is given by Equation 8. In this circuit-based analysis an “elementary circuit” consists of two infinitesimal-width transverse conducting strips separated by a half-wavelength and shorted at their ends by shorting means of “zero” resistance and inductance. The laminated track then consists of a stack of planar sheets, each such sheet being made up these elementary circuits so as to form the slotted surface that characterizes the laminated track

$$\begin{aligned} \phi(t) &= -\left(\frac{2B_0}{k}\right) \{ [(w_U - w_L) \text{Exp}[-k(y_1 - y)] - w_L (\text{Exp}[-k(y_1 - y)] - \text{Exp}[-k(y_1 + y)])] \} \text{Sin}[\omega t] \quad (8) \\ &= \phi_0 \text{Sin}(\omega t) \end{aligned}$$

Here  $\omega = kv$  is the angular frequency of the flux generated by the moving Halbach array.

The time-varying current induced in an elementary circuit of the laminated track, given by Equation 9, is calculated from circuit theory.

$$I(t) = \frac{\phi_0}{L_c} \left[ \frac{1}{1 + (R_c / \omega L_c)^2} \right] \left[ \text{Sin}(\omega t) + \left( \frac{R_c}{\omega L_c} \right) \text{Cos}(\omega t) \right] \quad (9)$$

Here  $L_c$  (henrys) and  $R_c$  (ohms) are the inductance and resistance of the elementary circuit defined above.

The levitation force at  $x = 0$  on an elementary circuit,  $F_y$  (Newtons), equal to the product of the  $x$  component of the magnetic field and the current, is given by Equation 10.

$$F_y = [(w_U - w_L) \sum B_{x2}(x=0, y) + w_L \sum B_{x1}(x=0, y)] I(t) \quad (10)$$

Similarly, the drag force,  $F_y$ (Newtons) at  $x = 0$  associated with the induced current,  $I(t)$ , is given by the product of the  $y$  component of the magnetic field and the current as shown in Equation 11. (The additional drag force component associated with parasitic eddy currents in the conducting strips of the laminated track will be considered later.)

$$F_x = [(w_U - w_L) \sum B_{y2}(x=0, y) + w_L \sum B_{y1}(x=0, y)] I(t) \quad (11)$$

Inserting the definitions of the above quantities and performing a time average yields equations for the steady-state lift and drag forces on an elementary circuit. If we now consider a single sheet of the laminated track made up of these elementary circuits, with a spacing  $d_c$ (m) between the center lines of each conducting strip, we then can obtain, after some algebraic simplifications, expressions for the lift and drag forces per unit area (i.e. per  $m^2$ ) on such a sheet, as given by Equations 12 and 13.

$$\frac{\langle F_y \rangle}{\text{Area}} = \frac{B_0^2 w_U}{k L_c d_c} \left[ \frac{1}{1 + (R_c / \omega L_c)^2} \right] \text{Exp}[-2k(y_1 - y)] \{1 - (w_L / w_U)^2 \text{Exp}(-4ky)\} \quad (12)$$

$$\frac{\langle F_x \rangle}{\text{Area}} = \frac{B_0^2 w_U}{k L_c d_c} \left[ \frac{(R_c / \omega L_c)}{1 + (R_c / \omega L_c)^2} \right] \text{Exp}[-2k(y_1 - y)] \{1 - (w_L / w_U) \text{Exp}(-2ky)\}^2 \quad (13)$$

Thus far the only significant approximation that has been made is the use of the truncated 2-D Halbach array field equations in calculating the lift and drag forces. We have also thus far left undefined the resistance and inductance terms. For the inductance of an elementary circuit embedded in an array of other circuits so as to form a sheet of the laminated track we will employ a definition of the “distributed inductance”,  $L_d$  (Henrys), as derived by Ryutov [3], employing a theoretical model based on surface currents. Thus for each leg of an elementary circuit we will assign the value given by Equation (14).

$$L_d = \frac{\mu_0 w_c}{2k d_c} \quad \text{henrys} \quad (14)$$

Here  $\mu_0 = 4\pi \cdot 10^{-7}$  henrys/meter, and  $w_c$  (m) = length of the strip conductor of the elementary circuit. The total inductance of an elementary circuit is thus twice the value of  $L_d$ . When this definition is inserted into Equations 12 and 13 there results the expressions for the lift and drag forces given by Equations 15 and 16.

$$\frac{\langle F_y \rangle}{\text{Area}} = \frac{B_0^2 w_U}{\mu_0 w_c} \left[ \frac{1}{1 + (R_c / \omega L_c)^2} \right] \text{Exp}[-2k(y_1 - y)] \{1 - (w_L / w_U)^2 \text{Exp}(-4ky)\} \quad (15)$$

$$\frac{\langle F_x \rangle}{\text{Area}} = \frac{B_0^2 w_U}{\mu_0 w_c} \left[ \frac{(R_c / \omega L_c)}{1 + (R_c / \omega L_c)^2} \right] \text{Exp}[-2k(y_1 - y)] \{1 - (w_L / w_U) \text{Exp}(-2ky)\}^2 \quad (16)$$

We are now ready to introduce the next important approximation used to obtain the final expressions for the lift and drag forces, the equations that will be used to program the levitation code used at Livermore for modeling Inductrack II systems and to be bench-marked against the experimental results from the Laminated Track Test Rig.

To determine a value for the total lift and drag forces (except for the drag from parasitic eddy currents, to be discussed later) arising from a laminated track composed of many thin slotted sheets we will introduce the “equivalent conductor” concept. In employing this concept we first visualize a single sheet conductor located at a specific value of  $y$  within the upper and lower boundaries of the stack of laminations. The circuit inductance of this sheet is calculated using Equation 14 and its circuit resistance is the resistance value one would obtain from conductors whose width is  $d_c$  and whose thickness in the vertical direction is equal to the thickness of the laminate stack. In this way we determine lift and drag forces associated with the particular value of  $y$  that has been chosen, when exposed to the vertical flux component given by Equation 8. We then conceptually place this “equivalent conductor” at all the values of  $y$  within the laminate stack and perform an (numerical) integral-average of these values. The end result is a calculation of the total lift and drag forces that would be exerted under the assumption that the incident fields at a given  $y$  value are not appreciably perturbed by the currents induced in adjacent sheets.

The latter approximation clearly needs justification as to its domain of validity. First, if the conducting strips of each lamination are very narrow compared to a skin depth, and their thickness is also very small compared to a skin depth the presence of parasitic eddy currents in one sheet will make a negligible perturbation to the flux from the Halbach arrays passing through an adjacent sheet. Second, if the length of the conducting strips,  $w_c$ , is much greater than the widest dimension of the Halbach array,  $w_U$ , then the inductance of each elementary circuit will so limit the induced current that there will be a negligible perturbation of the flux incident on a given lamination caused by the currents induced in laminate sheets above or below that sheet.

As it turns out, for track and Halbach array parameters of interest, and in particular for the parameters employed in the Laminated Track Test Rig, the “equivalent conductor” approximation gives results that are in good agreement with the experiment. Certainly one must always be aware of the domain restrictions on the approximations that have been made, using the more rigorous “fields-based” treatment described in other parts of this paper as a check. Nevertheless, and particularly for scoping designs and for inter-comparison of options, the fast-computing code that we have developed employing these approximations has proved to be a valuable tool.

## 2.2 Parasitic eddy-current losses

To complete the discussion of the 2-D levitation code as applied to the laminated track the effect of parasitic eddy-current losses in the conducting strips of the track needs to be considered. A simple derivation can be used to show that the two sources of drag losses (levitating currents and parasitic eddy currents) can be considered independently and then summed to determine the total drag.

Parasitic eddy current losses arise owing the incidence of a time-varying magnetic field normal to the surface of a conducting strip. The effect is to create a pattern of counter-flowing currents in

the strip, but no net current. The eddy current losses are thus simply the ohmic losses in the conductor associated with these parasitic currents. These losses scale down rapidly (as the cube) with the width of the conducting strip in the direction normal to the field, so that this scaling provides a means for limiting the eddy current losses so that they are acceptably small.

The expression for the parasitic eddy current losses in Watts/meter length of a conducting strip with a width  $w$ (m), a thickness,  $t$ (m) and a resistivity,  $\rho$  (ohm-meters), when exposed to a time varying magnetic field,  $B$ , incident normal to the “ $w$ ” face is given by Equation (17).

$$\frac{P}{\text{length}} = \frac{1}{24} \frac{\omega^2 B^2 t w^3}{\rho} \quad \text{Watts/meter} \quad (17)$$

This expression was programmed into the Laminated Track Levitation Code, using the same truncated 2-D fields employed to calculate lift and drag. The (weaker) perpendicular field is, of course, incident normally on the conducting strips of the track, while the (stronger) horizontal field component is incident on the thickness dimension of the strip, which is therefore made much thinner than the width of the conducting strips.

### 2.3 Check of the validity of the use of truncated 2-D fields in the levitation code

In order to estimate the errors associated with the use of truncated analytic 2-D functions for the representation of the real 3-D fields from the Halbach arrays another code was written, again using the Mathematica® platform. The ability of that platform to handle complicated double integrals analytically allowed the programming, analytically, of the magnetic field components of a rectangular bar magnet polarized at an arbitrary angle transverse to a reference face, and located at an arbitrary position on a reference plane. Then using this analytic representation a Halbach array of arbitrary order and physical dimensions can be built up. The end result: a very fast-computing code that can be used to determine the field components, at an arbitrary location, from Inductrack I or Inductrack II configurations. Other than the assumption of fixed Amperian currents to represent the permanent-magnet bar fields and the use of the Biot-Savart law in calculating the fields from the bars no simplifications or approximations were used.

In exercising the 3-D field code and comparing its computed fields with those determined using the 2-D analytic formulation of Halbach there were some pleasant surprises. In the context of an Inductrack system that uses a laminated track that is wider than the width of the Halbach array (as would be the case in most practical applications), the effect of the “fringing fields” produced by the Amperian currents flowing transversely at the ends of each Halbach array bar is to compensate, very nearly, for the fall-off of the field occurring upon approaching the edges of the Halbach arrays that are perpendicular to the direction of motion down the track. Also, the decrease in field (relative to the truncated 2-D analytic field) observed in the front and back ends of the array is relatively small. Figure 1 illustrates this latter point, a plot of  $B_z$  vs  $x$ , at a distance of .0225 m. from the upper array, for an  $M=8$ , “(5 x 3),” dual Halbach array with the following magnet parameters:

Remanent field	1.4 Tesla
Number of magnet bars per array	25
Length of upper magnet bars	0.25 m.
Length of lower magnet bars	0.15 m
Height of bars	0.025 m.
Width of bars	0.025 m.
Wavelength of M= 8 Halbach arrays	0.4 m

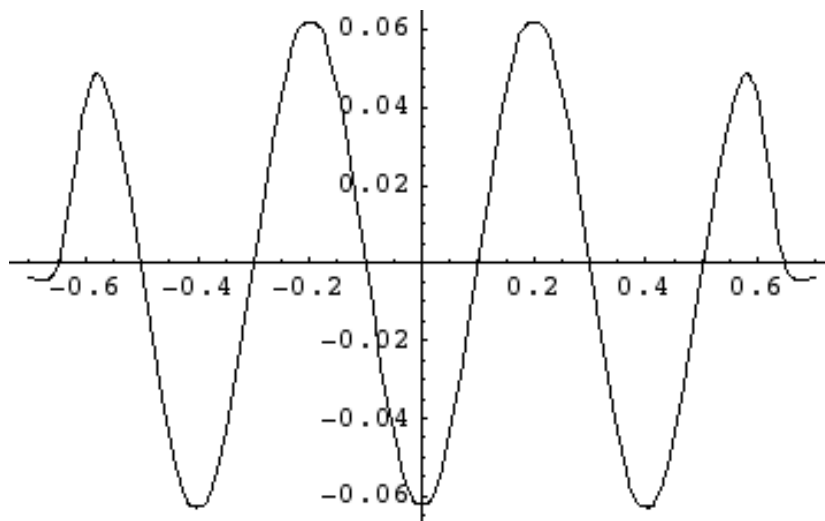


Figure 1: Plot of calculated  $B_z$  as a function of  $x$  for  $z = 0$  and gap ( $y$ ) = .035 m.

Note that of the seven maxima in  $B_z$ , five of the maxima have essentially full amplitude. Also note that the array that was calculated is shorter in the longitudinal ( $x$ ) direction than arrays, such as those used in the General Atomics designs [2] so that in those designs these end effects would be even further reduced.

When a “(5 x 3)” configuration was modeled the 3-D code yielded very useful information on the question: How well does the 2-D levitation code model reality? A test of this reality is to compare the value of the integrals, in the transverse direction, of the peak  $B_z$  and peak  $B_x$  values, and then compare these values with those calculated by multiplying the 2-D component by the width of the Halbach arrays. To take into account the (here) helpful effect of the 3-D fringing fields the integrations are carried out for a distance on each side of the Halbach array equal to 50 percent of the transverse width of the array. It is to be expected that in most applications of the laminated track the slots will be at least as wide as the width over which the integrations were performed. Table I summarizes the comparisons just described.

**Table I**

Integral of $B_z$ (peak) $\underline{vs}$ $z$ , for $-w < z < w$ :	0.1068 Tesla-meters
Product of $B_z$ (2-D, peak) and $w$	0.1071
Integral of $B_x$ (peak) $\underline{vs}$ $z$ , for $-w < z < w$	0.1044
Product of $B_x$ (2-D, peak) and $w$	0.1071

As can be seen from the table these pairs of evaluations (which are representative of the inducing flux and the levitating force) differ by only a percent or two. Also encouraging is the fact that the peak fields themselves, i.e. those located midway between the sides of the array and at a maximum in the  $x$  direction, differ by less than a percent from the 2-D-calculated value.

To illustrate the type of detail that the 3-D is capable of providing, Figure 2 is a 3-D plot produced by the code showing the magnitude of the  $B_z$  field component midway between the upper and lower Halbach arrays of a “(5 x 3)” Inductrack II,  $M = 8$ , configuration made up of magnet bars with the dimensions given above.

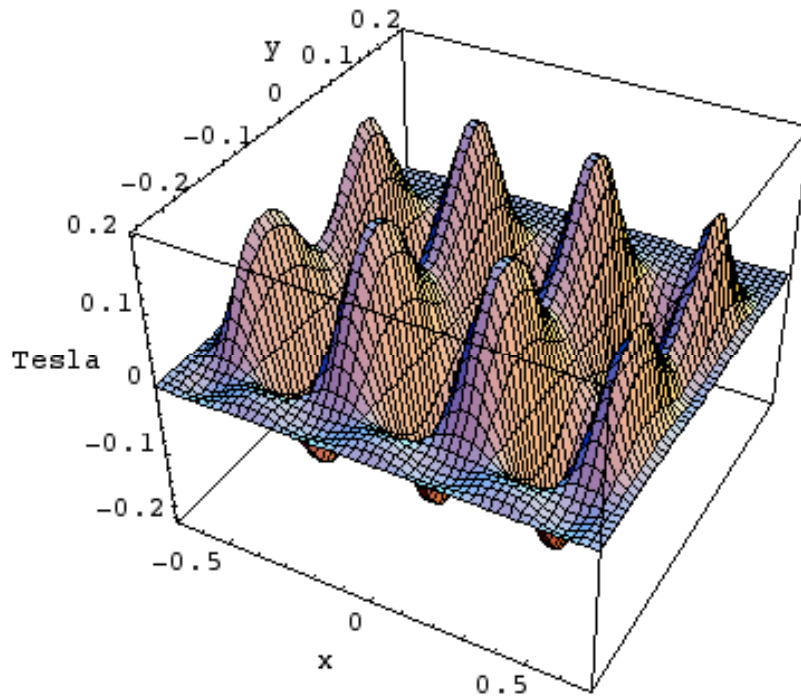


Figure 2: 3-D plot of magnitude of  $B_z$  at midplane of a  $M=8$ , “5 x 3” Inductrack II array

We conclude, based on the comparisons given above, that as far as the integrated magnetic fields are concerned, the lift and drag forces calculated using the 2-D truncated values should differ little, in typical cases, from the 3-D values calculated from first principles.

### 3 Laminated Track Test Rig

The Livermore Laminated Track Test Rig was designed and built to provide an experimental check on the laminated-track computer code calculations and to help build a data base for designing a laminated track system. The use of this rig enables making measurements, as a function of velocity, of the lift, drag, and stiffness coefficients of a laminated track interacting with both single (Inductrack I) and double Halbach array (Inductrack II) configurations. In the test rig a section of laminated track is pulled (on precision guide rails) through a Halbach array assembly and mount that is instrumented to measure the lift and the drag forces. The critical dimensions of the test rig, i.e., wavelength of the Halbach arrays, and the thickness of the laminated track, are scaled down by a factor of four from a full-size system. As a result the data that are taken can be extrapolated to a full-size system by using known scaling laws. By moving the track instead of the Halbach arrays, and by using pressure sensors with near-zero displacement under load, all inertial and displacement-sensitive corrections to the forces are eliminated, simplifying data reduction and improving the experimental accuracy.



Figure 3: Test rig

Figure 3 is a photograph of the test rig, showing the assembly that holds the Halbach array and the vertical force sensor, together with the carrier for the laminated track elements, propelled through the Halbach arrays by a gravity-driven pulley-and-weight system (not shown).

The track itself is made up of a stack of 0.5 mm thick copper sheets. The sheets are 20 cm. wide and the slots in the sheet are 15 cm. wide, leaving “shorting” strips at each end that are 2.5 cm. in width. The slots, made by chemical etching, using printed circuit techniques, are 0.5 mm wide, and the thus-formed strip conductors between them are 2.5 mm. wide. For the measurements reported here the laminate stack was 10 sheets thick. Longitudinally the track was made of three

such stacks, each approximately 75 cm. long. The stacks were butted together at their ends but no provision was made for longitudinal electrical conduction continuity of the track at the butt joints.

The stacks were mounted on a carrier “cart” that was equipped with v-grooved rollers that were captured between precision-ground guide rails, insuring accurate vertical and horizontal positioning of the cart. Since the peak forces exerted by the Halbach arrays on the track were large (100 kilograms or more) the rollers were spaced at many locations along the cart and additional support against vertical displacements was provided by rubber-tired rollers located so as to engage the cart as it passed through the Halbach-array mounting structure. Even with these precautions local deflections of a fraction of a millimeter occurred in some situations, leading to measurement errors that were, however, deemed to be acceptably small upon analysis of the data and the computer-code results.

As previously noted, the choice to move the track under stationary Halbach arrays rather than vice-versa was based on the consideration that the force measurements could be made without any influence from inertial effects, since “zero-displacement” force sensors could be used. Based on previous experience our choice was to use spring-loaded hydraulic pistons equipped with solid-state pressure sensors for the force measurements. To measure the velocity of the track as it moved through the Halbach array assembly we employed a tachometer generator attached to a rubber-edged wheel that engaged the edge of the cart as it moved by. Both systems worked well in the experiments.

The track was propelled through the Halbach arrays by a flexible stainless-steel cable that was tensioned by a gravity-driven pulley-and-weight system. The design of the drive system was based on a simple analytical formula for such systems. In order to achieve adequate acceleration, i.e., to accelerate the cart (weight about 50 kilograms), to velocities of order 10 meters/second in the available distance of 4 meters, accelerations of order 1.0 g are required. As the analysis showed, accelerations this high can only be obtained in a gravity-driven system by using a multi-cable system, in our case a four-pulley, four-cable system. The driver weight consisted of a stack of lead bricks loaded onto a carrier attached to the end of the steel cable.

The equation governing the velocity achieved by the load mass,  $M_L$  after an acceleration distance of  $s_L$  (meters) is the familiar one given by Equation (18).

$$v_s = \sqrt{2a_L s_L} \quad \text{meters / second} \quad (18)$$

The acceleration term,  $a_L$  ( $\text{m}/\text{sec}^2$ ) is determined by the driving mass,  $M_d$ , the load mass,  $M_L$ , and the number of supporting cables,  $N$ , of the pulley and weight system. Defining the ratio  $M_d/M_L = K$ , the acceleration is given by Equation (19).

$$a_L = \frac{K/N}{1+K/N^2} g \quad \text{meters / sec.}^2 \quad (19)$$

In setting up the system a calibration run was made to compare the measured cart velocities with those predicted by Equations (18) and (19). Figure 4 is a plot of the results of this run, showing good agreement between the theory and the measured velocity.

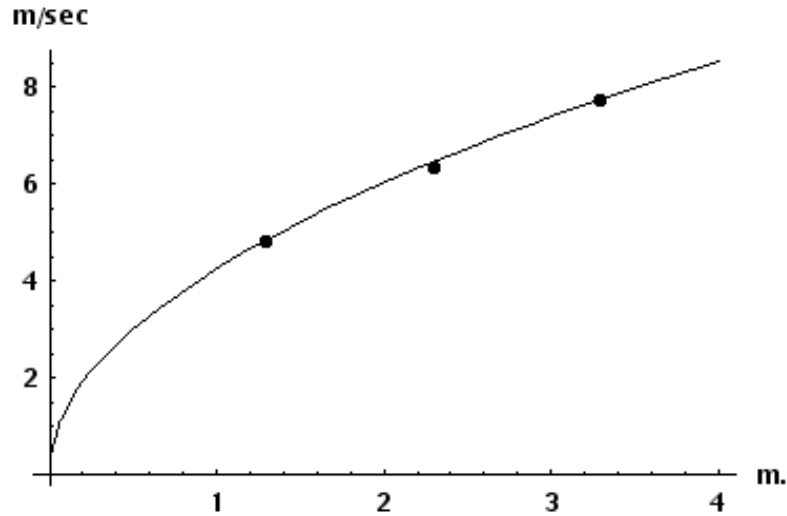


Figure 4: Comparison between theoretically predicted cart velocity and tachometer-wheel velocity measurements. Cart mass = 45 kg., driver mass = 220 kg. ( $K = 4.9$ ). Axes: x (starting point in meters); y (velocity, m/sec).

We report here the results of measurement of a "(5 x 3),"  $M = 4$ , array made up of blocks of NdFeB magnet material ( $B_r = 1.2$  Tesla) with dimensions 2.5 cm x 2.5 cm x 1.25 cm. The wavelength of the Halbach arrays was 10 cm. and the length of the array in the x direction was 4.0 wavelengths (plus a slight overhang at each end to partially compensate for end effects).. The width of the upper array was 5.0 cm and that of the lower array was 3.0 cm. The gap between the upper and lower arrays was 3.5 cm.

Figure 5 and 6 show comparison plots between the lift and drag force as calculated by the Livermore levitation code (based on the 2-D and other approximations discussed above) and the results from the Laminated Track Test Rig. In the plots the upper and lower curves shown bracketing the middle plotted curve represent the effect of a displacement of 1.0 mm up or down relative to the nominal gap position. The plots pointed are the results of measurements taken at different speeds of transit of the track through the Inductrack II dual Halbach array. The scatter of data observed, corresponding to a fraction of a mm of displacement, are of the order of that reasonably could be expected to arise from vibrational displacements and track fabrication inaccuracies.

On the basis of the above comparisons, and others made with different Halbach array configurations (to be reported at a later time), we conclude that the 2-D-based code is capable of giving predictions that can be employed in performing design studies of full-scale laminated track systems. The code should therefore be useful for such purposes when backed up by calculations made using the rigorous treatment described in Section 4 of this paper.

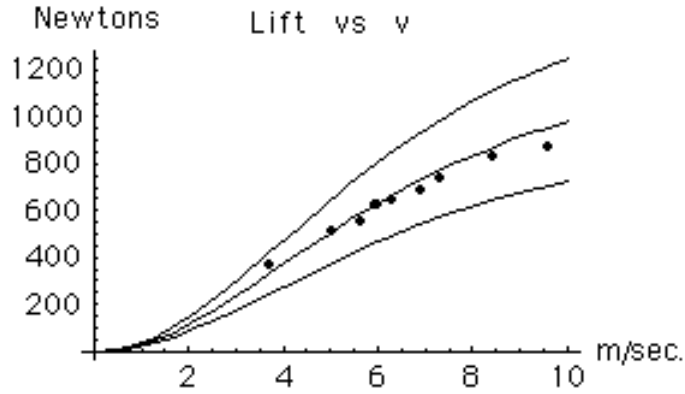


Figure 5: Comparison between lift force predictions of the Livermore 2-D levitation code and measurements made with the Livermore Laminated Track Test Rig performed on a 5 x3 Inductrack II Halbach array configuration.

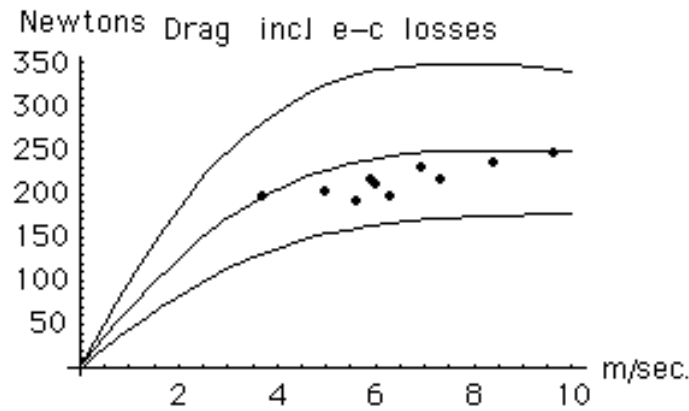


Figure 6: Comparison between drag force predictions of the Livermore 2-D levitation code and measurements made with the Livermore Laminated Track Test Rig that were performed on a 5 x3 Inductrack II Halbach array configuration.

#### 4 Fields-based analytic description

We describe here an analytic model that, in contrast to the “circuits-based” description of Section 2, is developed directly in terms of the 3-D fields of the permanent magnets, along with 2-D fields from the induced currents in the individual laminations of the track. This model differs from the circuits-based model in two ways: (1) it uses a Fourier analysis of the 3-D source fields in the direction of vehicle motion, with retention of the first Fourier component, to explicitly determine the nature of the “2 ½ -D” approximation, and (2) it accounts directly for the mutual coupling between the laminations by including contributions to the fields that penetrate and interact with each lamination in the matrix equation that governs the induced currents.

The fields-based model shown in Figure 7 describes the mutual coupling between upper and lower Halbach arrays and any number (3 are shown in the figure) of passive conducting layers between the two sources.

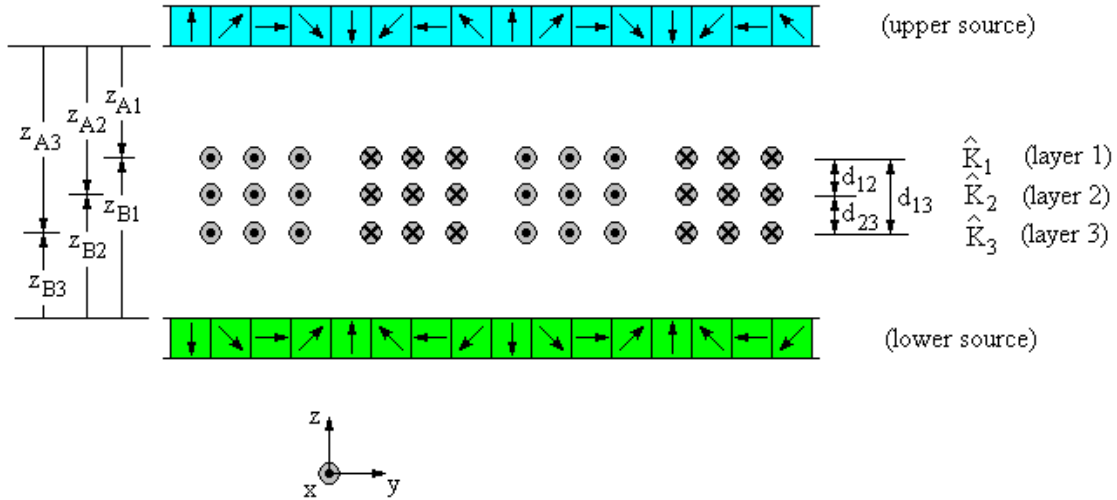


Figure 7: A model that accounts for 2-dimensional induced currents in laminations, including mutual coupling, and 3-dimensional source fields.

In a simple 2-dimensional model, the source fields as well as the fields due to induced currents in the laminations take the form of traveling waves. However, in order to account for the transverse (3-dimensional) structure of the source fields, we use the fundamental Fourier component of the source fields at each transverse ( $x$ ) position, and integrate these Fourier components over the track width to find the total source flux that passes through each lamination.

Figure 8 shows longitudinal ( $y$ ) and vertical ( $z$ ) components of the source magnetic flux density over a plane within one lamination for the double Halbach array that is 5 magnets wide in the upper array and 3 magnets wide in the lower array, as described in Section 2. The components on the left in Figure 8 are calculated on the basis of superimposing contributions from individual magnet cubes in the arrays, using either a magnetization current or magnetization charge methodology [4]. The components on the right are based upon retaining only the first term in a Fourier series representation of the fields at each widthwise ( $x$ ) position. The first Fourier component provides a relatively accurate description of the source field structure, including widthwise variations, in a form that is amenable to a sinusoidal steady state phasor analysis of the resultant induced currents in the laminations.

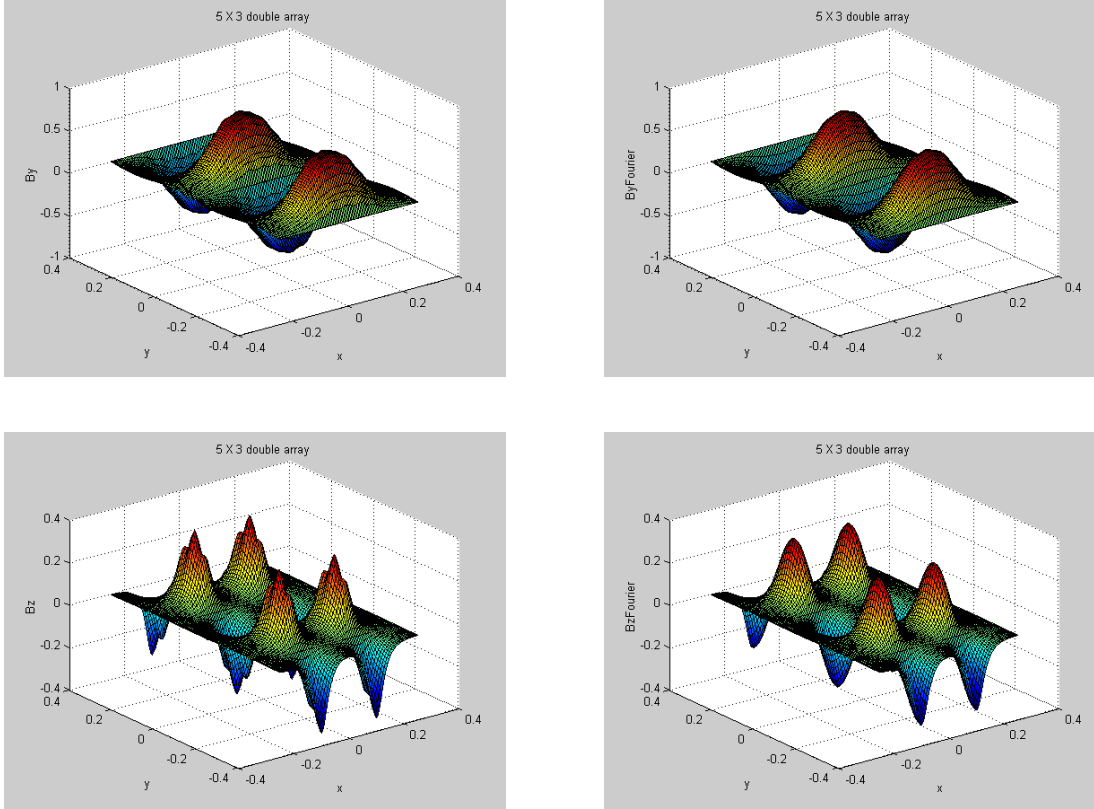


Figure 8: Longitudinal (top) and vertical (bottom) magnetic field components as calculated from individual magnet cube contributions (left) and only first Fourier component at each widthwise position (right).

A self-consistent description of the induced currents in the laminations, including mutual coupling, is accomplished as follows:

With the source wavelength denoted  $\lambda$  and with the velocity of the source relative to the track denoted  $v$ , the induced current in each layer is described by as a surface current that takes the form of a traveling wave:

$$\bar{K} = \bar{i}_x \operatorname{Re} \left\{ \hat{K} \exp \left[ j \frac{2\pi}{\lambda} (vt - y) \right] \right\}. \quad (20)$$

Each lamination contributes fields above and below itself that have a Laplacian character, with exponential decays in the vertical direction based upon wavelength in the longitudinal direction.

The 2-dimensional descriptions of currents and fields are quite accurate, because the thin, slotted laminations force induced currents to take this form over most of their widths – it is only at the outside edges of the laminations beyond the slots that the current paths become more complicated, and even there, they have no vertical components.

Faraday's Law governs induced currents in each lamination, and is written for a rectangular contour that is one-half wavelength long. In the sinusoidal steady state, the following complex amplitudes describe the coupling between physical variables at the vertical position of any one lamination:

$\hat{E}_x$ :	widthwise induced electric field
$\hat{\Lambda}_A$ :	total flux from upper array that passes through contour
$\hat{\Lambda}_B$ :	total flux from lower array that passes through contour
$\hat{\Lambda}_{self}$ :	total flux from induced current in lamination being described
$\sum \hat{\Lambda}_a$ :	total flux from laminations above lamination being described
$\sum \hat{\Lambda}_b$ :	total flux from laminations below lamination being described

Using  $\ell$  to denote the width over which induced currents circulate and  $p$  to denote the "packing fraction" in the longitudinal direction of conducting strips with interspersed slots in each lamination, we write Faraday's Law:

$$2\ell\hat{E}_x = -j\omega\left[\hat{\Lambda}_A + \hat{\Lambda}_B + p\left(\hat{\Lambda}_{self} + \sum \hat{\Lambda}_a + \sum \hat{\Lambda}_b\right)\right] \quad (21)$$

where, for laminations with conductivity  $\sigma$  and thickness  $\Delta$ , the complex amplitudes of induced electric field and surface current density are related by:

$$\hat{E}_x = \frac{\hat{K}_x}{\sigma\Delta} \quad (22)$$

Writing the fluxes through each rectangular loop in terms of the surface currents that serve as their sources, we form a system of self-consistent equations that determine the induced surface current densities, with source terms that are based upon integrals over the track width of the array field complex amplitudes. The solution involves the product of the source frequency

$\omega = 2\pi\frac{v}{\lambda}$ , based upon the vehicle velocity and wavelength, with a magnetic diffusion time

defined by  $\tau_m = \frac{\mu_0\sigma\Delta\lambda}{4\pi}$ .

The system of equations takes the form:

$$\begin{bmatrix}
\left(1 + \frac{1}{j\omega p \tau_m}\right) & e^{-kd_{12}} & e^{-kd_{13}} & \dots \\
e^{-kd_{12}} & \left(1 + \frac{1}{j\omega p \tau_m}\right) & e^{-kd_{23}} & \dots \\
e^{-kd_{13}} & e^{-kd_{23}} & \left(1 + \frac{1}{j\omega p \tau_m}\right) & \dots \\
\dots & \dots & \dots & \dots
\end{bmatrix}
\begin{bmatrix}
\hat{K}_1 \\
\hat{K}_2 \\
\hat{K}_3 \\
\dots
\end{bmatrix}
= \frac{j2}{p\ell}
\begin{bmatrix}
\int_{-\ell/2}^{\ell/2} \hat{H}_z^A(x, z_{A1}) dx + \int_{-\ell/2}^{\ell/2} \hat{H}_z^B(x, z_{B1}) dx \\
\int_{-\ell/2}^{\ell/2} \hat{H}_z^A(x, z_{A2}) dx + \int_{-\ell/2}^{\ell/2} \hat{H}_z^B(x, z_{B2}) dx \\
\int_{-\ell/2}^{\ell/2} \hat{H}_z^A(x, z_{A3}) dx + \int_{-\ell/2}^{\ell/2} \hat{H}_z^B(x, z_{B3}) dx \\
\dots
\end{bmatrix}
\equiv \frac{j2}{p\ell}
\begin{bmatrix}
\hat{I}_z^1 \\
\hat{I}_z^2 \\
\hat{I}_z^3 \\
\dots
\end{bmatrix}
\quad (23)$$

After the induced currents are determined by solving these matrix equations, the time-averaged forces on the sources are computed.

The time-averaged lift force per wavelength is:

$$L_\lambda = -\frac{\mu_0 \lambda p}{2} \sum_i \operatorname{Re} \left\{ \int_{-\ell/2}^{\ell/2} \hat{K}_i^* [\hat{H}_y^A(x, z_{Ai}) + \hat{H}_y^B(x, z_{Bi})] dx \right\} \equiv -\frac{\mu_0 \lambda p}{2} \sum_i \operatorname{Re} \{ \hat{K}_i^* \hat{I}_y^i \} \quad (24)$$

and the time-averaged drag force per wavelength is:

$$D_\lambda = -\frac{\mu_0 \lambda p}{2} \sum_i \operatorname{Re} \left\{ \int_{-\ell/2}^{\ell/2} \hat{K}_i^* [\hat{H}_z^A(x, z_{Ai}) + \hat{H}_z^B(x, z_{Bi})] dx \right\} \equiv -\frac{\mu_0 \lambda p}{2} \sum_i \operatorname{Re} \{ \hat{K}_i^* \hat{I}_z^i \} \quad (25)$$

Application of this methodology to the LLNL laminated track test rig produces lift and drag as functions of vehicle velocity as shown in Figure 9 for track positions that are centered and displaced by 1 mm up and down with respect to the upper and lower portions of a “5 X 3” double

Halbach array. The curves are in excellent agreement with the LLNL experimental measurements, and with the LLNL “circuits based” model.

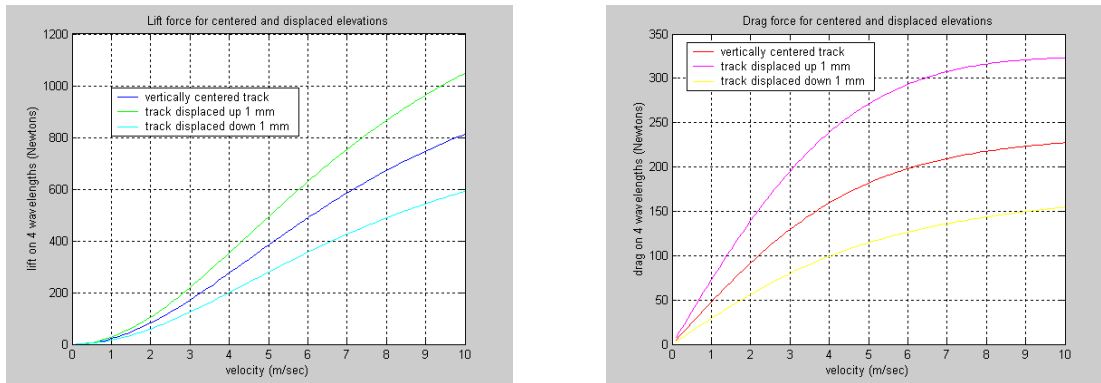


Figure 9. Lift and drag as functions of velocity for the LLNL “5 X 3” double Halbach array test rig.

## 6 Acknowledgements

The work of one of the authors (RFP) was performed under the auspices of the U. S. Department of Energy at the University of California Lawrence Livermore National Laboratory under contract W-7405-Eng-48.

This work was supported in part by the U.S. Department of Transportation, Federal Transit Administration Office of Technology, through General Atomics, under Cooperative Agreement No. CA-26-7025.

## 7 References

- [1] K. Halbach, Nucl. Inst. and Methods, **187**, 109 (1981)
- [2] S. Gurol, B. Baldi, R. F. Post, “Overview of the General Atomics Low Speed Urban Maglev Technology Development Program,” Proceedings of 17<sup>th</sup> International Conference on Magnetically Levitated Systems and Drives – “Maglev 2002,” Sept. 3-5, 2002, Lausanne, Switzerland
- [3] R. F. Post, D. D. Ryutov, “The Inductrack Concept: A New Approach to Magnetic Levitation,” Lawrence Livermore National Laboratory report UCRL-ID-124115. May 1996.
- [4] J. F. Hoburg, “Modeling Maglev Passenger Compartment Static Magnetic Fields from Linear Halbach Permanent Magnet Arrays,” *IEEE Transactions on Magnetics*, **40**, 1, January, 2004.